Therapeutics, Targets, and Chemical Biology

Cancer Research

Notch3 Pathway Alterations in Ovarian Cancer

Wei Hu[1], Tao Liu[1], Cristina Ivan[1,8], Yunjie Sun[1], Jie Huang[1], Lingegowda S. Mangala[1,8], Takahito Miyake[1], Heather J. Dalton[1], Sunila Pradeep[1], Rajesh Rupaimoole[1], Rebecca A. Previs[1], Hee Dong Han[1], Justin Bottsford-Miller[1], Behrouz Zand[1], Yu Kang[1], Chad V. Pecot[7], Alpa M. Nick[1], Sherry Y. Wu[1], Ju-Seog Lee[2], Vasudha Sehgal[2], Prahlad Ram[2], Jinsong Liu[3], Susan L. Tucker[5], Gabriel Lopez-Berestein[4,6,8], Keith A. Baggerly[5], Robert L. Coleman[1], and Anil K. Sood[1,6,8]

Abstract

The Notch pathway plays an important role in the growth of high-grade serous ovarian (HGS-OvCa) and other cancers, but its clinical and biologic mechanisms are not well understood. Here, we found that the Notch pathway alterations are prevalent and significantly related to poor clinical outcome in patients with ovarian cancer. Particularly, *Notch3* alterations, including amplification and upregulation, were highly associated with poor patient survival. Targeting *Notch3* inhibited ovarian cancer growth and induced apoptosis. Importantly, we found that dynamin-mediated endocytosis was required for selectively activating Jagged-1–mediated Notch3 signaling. Cleaved Notch3 expression was the critical determinant of response to Notch-targeted therapy. Collectively, these data identify previously unknown mechanisms underlying Notch3 signaling and identify new, biomarker-driven approaches for therapy. *Cancer Res; 74(12); 3282–93. ©2014 AACR.*

Introduction

Notch signaling has been implicated in tumor angiogenesis processes such as vessel maturation; pericyte recruitment; branching; and cell differentiation, proliferation, and survival. In mammalian cells, this pathway comprises five transmembrane Notch ligands [Jagged-1, Jagged-2, Delta-like ligand (DLL) 1, DLL3, and DLL4] and four Notch receptors (Notch1–4). Mature Notch receptors are assembled as heterodimeric proteins, with each dimer comprised of a large extracellular ligand-binding domain, a single-pass transmembrane domain, and a smaller cytoplasmic subunit (Notch intracellular domain, NICD; ref. 1). The activation of Notch signaling requires endocytosis and trafficking of both notch receptor and ligand. Upon ligand–receptor binding, it leads to cleavage of the Notch receptor *via* intramembrane proteolysis by the gamma-secretase complex (including pesenilin, nicastin, APH1 and PEN2) and results in consequent release of NICD. The NICD fragment then enters the nucleus and interacts with nuclear DNA-binding factor, CSL (suppressor of hailess/LAG-1, RBPJK) to regulate transcription of the basic helix-loop-helix genes, hairy and enhancer-of-split genes, and Notch target genes (2, 3).

However, the biologic role of Notch pathway alterations in cancer growth and the clinical effects of these alterations are not well understood (4–7). In the present study, we performed an integrated and systematic analysis of the clinical relevance of the Notch pathway in high-grade serous ovarian cancer (HGS-OvCa) and identified novel mechanisms of Notch3 activation.

Materials and Methods

The Cancer Genome Atlas clinical analysis

Access to The Cancer Genome Atlas (TCGA) database was approved by the National Cancer Institute. The University of Texas MD Anderson Cancer Center approved a waiver for performing our survival analysis with deidentified data. Demographic characteristics and clinical data of patients with HGS-OvCa (histopathologic information, treatment, and outcome parameters) were downloaded from the data portal for TCGA (http://tcga.cancer.gov; Supplementary Table S1).

The survival analysis output for the 316 study patients and complete information [overall survival (OS) and progression-free survival duration, expression, mutation, copy number] were downloaded from the cBio Cancer Portal for Genomics (http://www.cbioportal.org/public-portal/). Also, complete survival and gene expression information for our OS and progression-free survival analysis of 453 and 373 patients with HGS-OvCa, respectively, were downloaded from TCGA. The mean age of the patients at diagnosis and

Authors' Affiliations: Departments of [1]Gynecologic Oncology and Reproductive Medicine, [2]Systems Biology, [3]Pathology, [4]Experimental Therapeutics, [5]Bioinformatics and Computational Biology, [6]Cancer Biology, [7]Thoracic/Head and Neck Medical Oncology, and [8]The Center for RNA Interference and Non-Coding RNA, The University of Texas MD Anderson Cancer Center, Houston, Texas

Note: Supplementary data for this article are available at Cancer Research Online (http://cancerres.aacrjournals.org/).

W. Hu, T. Liu, and C. Ivan contributed equally to this work.

Current address for T. Liu: Department of General Surgery, Union Hospital, Tongji Medical College, Huazhong University of Science and Technology, Wuhan, Hubei, People's Republic of China.

Corresponding Author: Anil K. Sood, The University of Texas MD Anderson Cancer Center, 1155 Herman Pressler Street, Houston, TX 77030. Phone: 713-745-5266; Fax: 713-792-7586/713-792-3643; E-mail: asood@mdanderson.org

doi: 10.1158/0008-5472.CAN-13-2066

tumor stage (as defined by the International Federation of Gynecology and Obstetrics), tumor grade, and surgical outcomes (residual tumor size) reflected those in individuals typically diagnosed with HGS-OvCa. The patients' tumor specimens had been resected before systemic treatment. All the patients had received a platinum agent, and 94% had received a taxane. The platforms used were described in the TCGA article (4).

Copy-number alterations were analyzed using the Human Genome CGH Microarrays (244 k, 415 K, or 1 M platforms; Agilent Technologies), and focally amplified regions were identified using a modified method (4). Level 3 gene expression data were generated using three platforms: Agilent Technologies, GeneChip Human Exon ST Array (Affymetrix), and GeneChip Human Genome U133A 2.0 Array (Affymetrix). We downloaded the *Notch2–4* mutation data from TCGA (Supplementary Table S1); these data were generated using the Genome Analyzer IIx platform (Illumina) and the ABI SOLiD 3 System (Life Technologies/Applied Biosystems).

Cell lines and cell culture

Ovarian cancer cell lines (OVCAR3, OVCAR5, OVCAR420, SKOV3, SKOV3 TR, HeyA8, HeyA8 MDR, A2780, IGROV1, A2774, and HIO180) and the uterine cancer cell line (Ishikawa) were obtained from the MD Anderson Characterized Cell Line Core Facility (Houston, Texas), which supplies authenticated cell lines. The cell lines were routinely tested to confirm the absence of mycoplasma, and all experiments were performed with cell lines at 60% to 80% confluence.

OVCAR420, OVCAR3, SKOV3, SKOV3 TR, HeyA8, HeyA8 MDR, A2780, and IGROV1 cells were maintained and propagated in RPMI1640 medium supplemented with 10% to 15% FBS and 0.1% gentamicin sulfate (Gemini Bio-Products). The medium used for the HeyA8 MDR and SKOV3 TR cells contained 100 nmol/L docetaxel. OVCAR5 cells were maintained and propagated in Dulbecco's Modified Eagle Medium/high-glucose medium supplemented with 15% FBS and 0.1% gentamicin sulfate. HIO180 and A2774 cell cultures were maintained in 10% Modified Eagle Medium.

Reagents and antibodies

Gamma-secretase inhibitor (GSI) was provided by Pfizer (New York, New York). Paclitaxel was purchased from the MD Anderson pharmacy. Notch3, Jagged-1, RPS6KB1, dynamin (DNM)1–3, control siRNAs, and dynasore were purchased from Sigma-Aldrich. Primers included PSEN1, APH1A, NCSTN, APH1B, PSENEN, RPS6KB1, DNM1–3, and 18s were also purchased from Sigma-Aldrich. Antibodies used in this study included Jagged-1, Jagged-2, DLL1, DLL4, P70S6K (RPS6KB1), Notch1–4, and cleaved Notchs and were obtained from Cell Signaling Technology. Anti-DLL3 antibody was obtained from Abcam. β-Actin was purchased from Sigma-Aldrich. CD31 was purchased from BD Biosciences. Anti-Ki67 antibody was purchased from Neomarkers. Antibody against cleaved caspase-3 was purchased from Cell Signaling Technology. Horseradish peroxidase (HRP)–conjugated rat anti-mouse IgG2a was purchased from Harlan Bioproducts for Science.

Western blot analysis

Western blot analysis was performed to detect expression of Notch family members [Jagged-1, Jagged-2, DLL1, DLL3, DLL4, Notch1–4, and cleaved Notch (NICDs)] in a panel of ovarian cancer cells. Cells were lysed with RIPA lysis buffer (50 mmol/L Tris-cl pH 7.4, 150 mmol/L NaCl, 1% NP40, 0.25% Na-deoxycholate, 1 mmol/L PMSF (phenylmethylsulfonylfluoride), 1× Roche complete mini protease inhibitor cocktail) and centrifuged for 15 minutes at 4°C. Protein concentrations were then measured using a Bio-Rad Protein Assay Kit (Hercules, California). After loading the protein (25 μg/well), we separated bands on an 8% to 10% gel using sodium dodecyl sulfate polyacrylamide gel electrophoresis. Bands were then transferred to nitrocellulose membrane, blocked with 5% milk for 1 hour at room temperature, and incubated with primary antibodies against Notch1–4, Jagged-1, Jaged-2, and DLL4 (1:1,000 dilution) and DLL3 (1:2,000 dilution) overnight at 4°C. The samples were incubated with HRP-conjugated anti-mouse or anti-rabbit antibodies (GE Healthcare) for 1 hour at room temperature. Blots were developed using an enhanced Chemiluminescence Detection Kit (Pierce Biotechnology, Rockford, Illinois). Actin was used as a loading control, and all experiments were performed in duplicate. Densitometry was performed using the ImageJ software program to interpret differences in Western blot analysis results.

RT-PCR

Relative expression of the gamma-secretase complex (*PSEN1*, *NCSTN*, *APH1A*, *APH1B*, and *PSENEN*) were detected using qRT-PCR. Dynamin expression was detected using RT-PCR. Each RT-PCR was carried out with 500 ng of total RNA isolated from treated ovarian cancer cells using an RNeasy Mini Kit (Qiagen). Quantitative RT-PCR was performed using an ABI 7500 Sequence Detection System (Applied Biosystems) with a SensiMix SYBR Low-ROX Kit (Bioline USA). Relative quantification of gene expression was performed using the $2^{-\Delta\Delta C_t}$ method. The primer sequences are listed in Supplementary Table S2.

In vitro siRNA transfection

All cell lines were transfected with Lipofectamine 2000 reagent (Invitrogen) using either control or target siRNAs (Sigma-Aldrich) as specified in Supplementary Table S2 according to the manufacturer's protocol. Cells were plated in a 6-well plate 24 hours before incubation. For 1-well transfection, we added 2 μg of target siRNA (1 μg/μL) and 6 μL of Lipofectamine 2,000 to 100 μL of serum-free medium, and the mixture was incubated for 30 minutes at room temperature. During transfection, we washed the 6-well plates once with 2 mL of PBS and then added 100 μL of the mixture along with 1 mL of serum-free medium to the plates. After 4 to 6 hours of transfection, the medium was replaced with a medium containing FBS.

Apoptosis, cell cycle, and anoikis assays

Apoptosis in the ovarian cancer cells was evaluated using an Annexin V Apoptosis Detection Kit (BD Biosciences). Cells were incubated in trypsin-EDTA, and cell pellets were

suspended in 1 mL of 1× Annexin V binding buffer. We incubated 100 μL of each cell suspension with 5 μL of Annexin V and 5 μL of 7-aminoactinomycin D at room temperature (25°C) in the dark for 30 minutes. Following this incubation, 400 μL of 1× binding buffer was added to each tube, and specimens were analyzed using an XL 4-color flow cytometer. Each experiment was repeated three times.

For cell-cycle analysis, we synchronized the treated cells by maintaining them in serum-free media for 24 hours. The cells were then trypsinized, washed with PBS, and fixed in 70% cold ethanol overnight at 4°C. Cells were then centrifuged at 1,200 rpm for 10 minutes at 4°C. After washing with PBS, cells were suspended in propidium iodide (Roche Diagnostics) at 50 μg/mL and RNAse A (Qiagen) at 100 μg/ml and incubated in the dark at room temperature. We then determined the cell-cycle status using fluorescence-activated cell sorting.

For anoikis analysis, 2.0×10^5 ovarian cancer cells were seeded on a 6-well plate. Twenty-four hours later, cells were transfected with siRNA. After 24 hours of transfection, 2.5×10^5 cells were lifted and plated on a 6-well poly(2-hydroxyethyl methacrylate)-treated plate in serum-free mito-PLUS medium and incubated for 72 hours at 37°C in a 5% carbon dioxide atmosphere. After incubation, detached and suspended cells were harvested in RPMI1640 medium and centrifuged at 500 × *g* for 10 minutes. Pellets were washed with PBS and fixed with ice-cold 75% (v/v) ethanol overnight at 4°C. After fixation, cells were washed with PBS and stained with 500 μL of a propidium iodide solution (50 mg/mL in PBS) containing 25 μg/mL RNase A. Cells were incubated at 37°C for 30 minutes and analyzed using fluorescence-activated cell sorting.

Cytotoxicity assays

Ovarian cancer cells were plated in a 96-well plate and cultured overnight. Cells were then exposed to 0.25, 0.5, 1, 2, 4, 6, 8, or 10 μmol/L of GSI for 72 hours. Control cells were treated with a vehicle at equal concentrations. To assess cell viability, we added 50 μL of 0.15% MTT (Sigma-Aldrich) to each well and incubated the well-plate for 2 hours at 37°C. The medium containing MTT was then removed, and 100 μL of dimethyl sulfoxide (Sigma-Aldrich) was added to each well. Cells were then incubated at room temperature for 10 minutes. The absorbance was read at 570 nm using a 96-well Synergy HT multi-mode microplate reader (Ceres UV 900 C; BioTek). Cell viability was defined as the percentage of viable cells in the treatment group relative to viable cells in the control group. The experiments were repeated separately at least three times.

Microarray analysis of Notch3 downstream genes

We analyzed the silencing of *Notch3* with the Illumina cDNA microarray platform as described previously (8). Briefly, *Notch3* in OVCAR3 cells was silenced *in vitro* using *Notch3* siRNAs, and *Notch3* silencing was confirmed via Western blot analysis. For microarray hybridization, total RNA was extracted from ovarian cancer cells transfected with control siRNA or human *Notch3* siRNA using a mirVana RNA isolation labeling kit (Ambion). We used 500 ng of total RNA to label and hybridize the cells according to Illumina's protocols. After we scanned bead chips (Sentrix HumanHT-12 v3, Illumina) using an Illumina BeadArray reader, we normalized the microarray data using the quantile normalization method with the Linear Models for Microarray Data software program in the R language (Denton; ref. 9). The level of expression of each gene was transformed into a $\log_2$ base before additional analysis was performed. Genes that were differentially expressed in control and *Notch3*-silenced cells were identified using a random-variance *t* test; gene expression differences were considered statistically significant if their *P* values were less than 0.001. A stringent significance threshold was used to limit the number of false-positive findings.

In addition, cluster analysis was performed using the Cluster and TreeView software programs (10). The NetWalker software program was used for gene network analysis (11).

In vivo mouse models

Female athymic nude mice (*NCr-nu*) were purchased from the Animal Production Area of the Frederick National Laboratory for Cancer Research. The animals were kept under specific pathogen-free conditions in facilities approved by the Association for Assessment and Accreditation of Laboratory Animal Care International and in agreement with current regulations and standards of the United States Department of Health and Human Services, the United States Department of Agriculture, and the NIH. Mice used in these experiments were 8- to 12-week-old.

To generate tumors in the mice, we trypsinized subconfluent cultures of OVCAR5, A2780, and SKOV3 cells, mixed the cells with a medium containing 10% FBS, centrifuged the mixture at 1,000 rpm for 5 minutes, and washed the cells in PBS. Mice were then injected intraperitoneally with 1×10^6 OVCAR5, A2780, or SKOV3 cells. In the OVCAR5 and A2780 models, mice were randomized into four treatment groups of 10 mice each: control siRNA, control siRNA with paclitaxel, *Notch3* siRNA, and *Notch3* siRNA with paclitaxel. In the SKOV3 model, mice were randomized into two treatment groups: control siRNA and *Notch3* siRNA. Treatments were initiated 8 days after tumor cell injection. Control and *Notch3* siRNA were conjugated with chitosan (CH; ref. 8), which we injected into the tail vein twice weekly (150 μg/kg per mouse). Paclitaxel was administered intraperitoneally once weekly (4 mg/kg/mouse). Mice were monitored daily and weighed weekly. All of the mice were subjected to necropsy when the control mice became moribund, which was approximately 28 days after A2780 cell injection, 35 days after OVCAR5 cell injection, and 38 days after SKOV3 cell injection. Each mouse's total body weight and the location, weight, and number of tumors were recorded. Tumor specimens processed for further analysis were either preserved in optimum cutting temperature medium (Miles Laboratories; for frozen sectioning) or fixed in formalin (for paraffin embedment).

To further validate target modulation (cleaved Notch3, Hes1, and RPS6KB1) in the tumor tissues obtained from the *in vivo A2780* model, ovarian cancer cells were injected intraperitoneally into the mice. Three weeks later, the mice were randomly allocated to two treatment groups ($n = 5$/group): (i) control, (ii) dynasore (60 mg/kg i.p. for two treatments,

72 hours apart). Tumor tissues were collected for Western blot analysis.

Immunohistochemical staining

Paraffin-embedded orthotopic tumor specimens were used in immunohistochemical staining to detect cell proliferation (with Ki67), apoptosis (with cleaved caspase-3), and Notch3 expression. Tumor sections were deparaffinized, rehydrated, and transferred to PBS. After retrieving the antigens with citrate buffer (pH 6.0), we blocked the sections with 3% hydrogen peroxide in methanol and protein blocker at room temperature. The sections were then incubated with a monoclonal mouse anti-Ki67 antibody (1:200; Neomarkers), anti-Notch3 antibody (1:50; Santa Cruz Biotechnology), or anti-cleaved caspase-3 antibody (1:100; Biocare Medical) overnight at 4°C. After being washed with PBS, the sections were incubated with HRP-conjugated rat anti-mouse IgG2a (1:100; Harlan Bioproducts for Science).

For CD31 detection, frozen sections were fixed in cold acetone for 15 minutes, washed with PBS, blocked with protein blocker (4% fish gel), and then incubated with rat monoclonal anti-mouse CD31 (1:800; PharMingen) overnight at 4°C. They were then washed with PBS and incubated with HRP-conjugated goat anti-rat IgG (1:200, Jackson ImmunoResearch Laboratories) for 1 hour. Reactive tissues were visualized using staining with 3,3′-diaminobenzidine (Research Genetics) and followed by counterstaining with Gil hematoxylin (BioGenex Laboratories).

To quantify Ki67, cleaved caspase-3, and Notch3, the percentage of positive cells was determined in five random 0.159-mm^2 fields at ×200 magnification. To quantify microvessel density (MVD) for each sample, the microvessels within five randomly selected 0.159-mm^2 fields were counted at ×200 magnification. A single microvessel was defined as a discrete cluster for CD31 positivity.

Statistical analysis

The Kaplan–Meier method was used to generate time-to-progression and survival curves. The statistical analysis was performed with the R statistical computing language (version 2.11.0; http://www.r-project.org/), and statistical significance was set at 0.05. For analysis of categorical data (tumor stage, tumor grade, and residual tumor size), the Fisher exact test was used to calculate *P* values. For *in vivo* data analysis, differences in continuous variables (mean body weight, tumor weight, tumor-cell proliferation, and apoptosis) were analyzed using the Mann–Whitney rank-sum test.

Results

Clinical significance of alterations of the core Notch and related genes

To determine the clinical relevance of alterations of the core Notch and related genes, including Notch ligands (*Jagged-1*, *Jagged-2*, *DLL1*, *DLL3*, and *DLL4*), Notch receptors (*Notch1–4*), and Notch-interacting genes (*SNW1*, *CNTN1*), we first examined the effect of these alterations on survival duration in 316 patients with HGS-OvCa from the TCGA dataset. We found that *Notch3*, *DLL3*, *SNW1*, and *Jag1* were the genes altered (defined as amplification, upregulation or downregulation of expression, mutation, or homozygous deletion) most frequently (17%, 16%, 15%, and 9% of cases, respectively; Fig. 1A). In total, 61% of the HGS-OvCa cases had alterations of at least one of the Notch pathway–related genes. Patients with these alterations had shorter OS durations than did those without the altered genes (median, 36.2 vs. 53.2 months; $P = 0.001$; Fig. 1B). The types of alterations for each of the nine genes are shown in Fig. 1C. Notch pathway alterations were not significantly associated with other clinical parameters, including tumor stage (as defined by the International Federation of Gynecology and Obstetrics), grade, and residual tumor size (Supplementary Table S1A and S1C). Mutations of *Notch2–4* did not occur frequently in HGS-OvCa cases (Supplementary Table S1B), and there were no alterations in *Notch1* or *DLL1*.

We next focused specifically on *Notch3* due to its frequent alterations. Patients with *Notch3* alterations had significantly shorter OS durations than did patients without these alterations (median, 35.3 vs. 52.2 months; $P = 0.0005$; Fig. 2A). Furthermore, patients with amplification, increased expression, and mutation of *Notch3* genes had significantly shorter OS durations than did those without these alterations (median OS duration, 33.6 vs. 53.2 months; $P = 0.0014$; Fig. 2B). *Notch3* amplification alone was not associated with OS duration, but there was a trend of shorter OS duration in patients with amplification (Supplementary Fig. S1A). *Notch3* expression was correlated with its amplification ($P < 0.001$; Fig. 2C), according

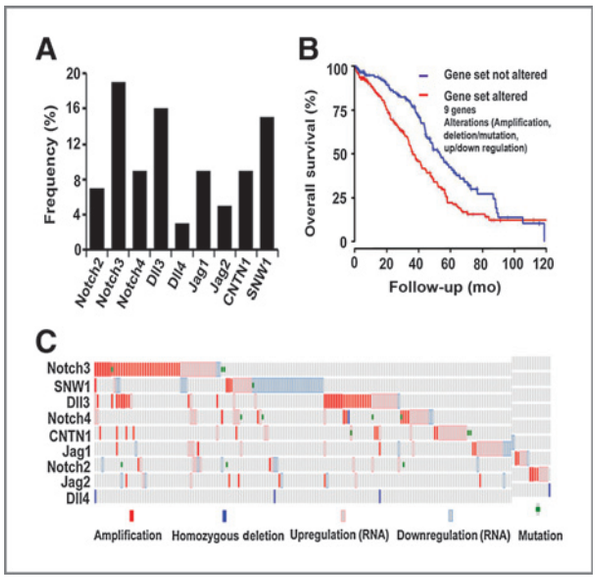

Figure 1. Alterations of Notch genes in patients with HGS-OvCa. A, frequency of alterations of nine Notch family genes and closely interacting genes. Among the alterations (amplification, upregulation and downregulation, mutation, and homozygous deletion), *Notch3*, *delta-like ligand (DLL)3*, *SNW1*, and *Jagged-1* were the most frequently altered genes (17%, 16%, 15%, and 9% of cases, respectively). B, OS durations in cases with and without gene alterations. The gene set consisted of *Jagged-1*, *Jagged-2*, *DLL3*, *DLL4*, *CNTN1*, *Notch2*, *Notch3*, *Notch4*, and *SNW1*. C, alteration patterns in the Notch signaling pathway. Each column represents an individual case with at least one alteration.

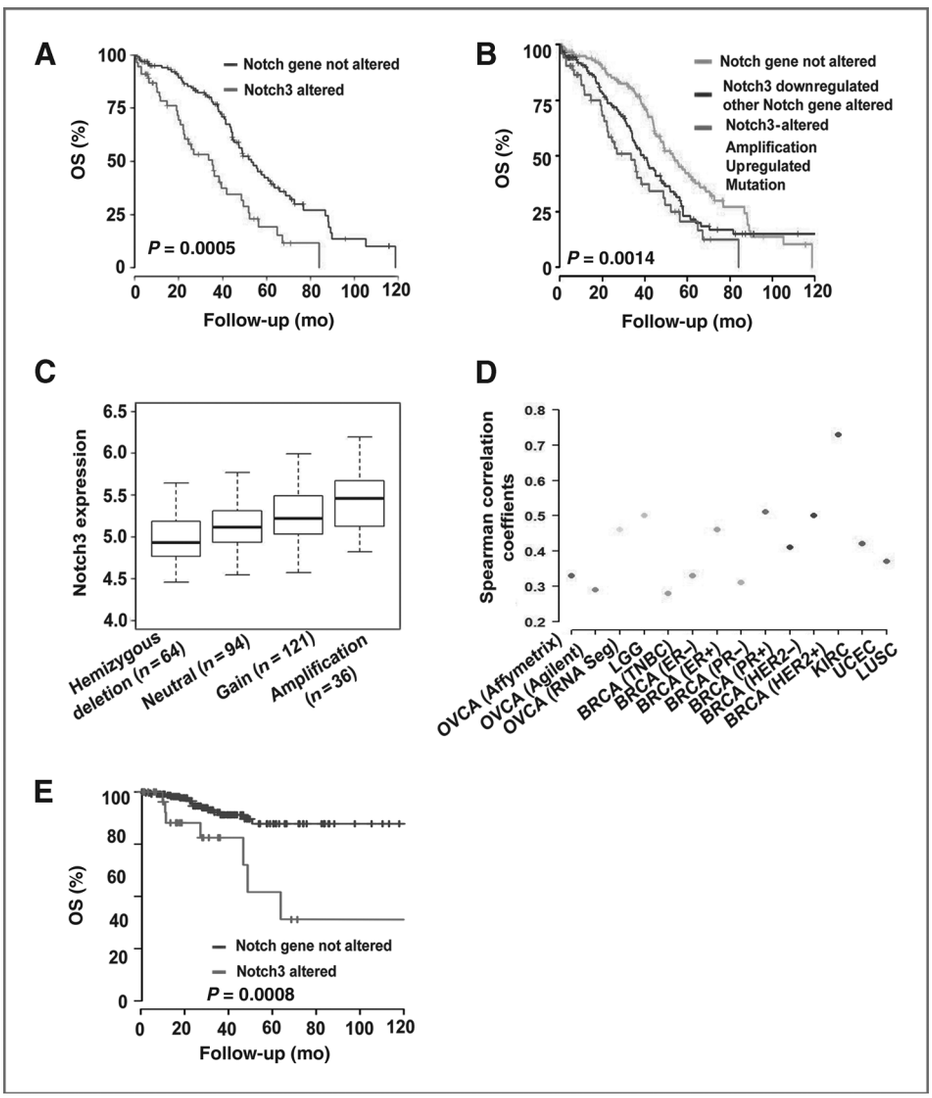

Figure 2. OS durations in patients with HGS-OvCa with *Notch3* alterations. A, OS durations in cases with and without *Notch3* alterations. B, OS durations in cases with amplified, upregulated, or mutated *Notch3* genes; with downregulated *Notch3* expression and alterations of other Notch genes; and without Notch gene alterations. C, correlation between Notch3 expression in patients with Notch amplification and in patients with gain, neutral, or hemizygous deletion of *Notch3*. D, correlation between Notch3 and Jag1 expression in human cancers. LGG, brain low-grade glioma; BRCA, breast invasive carcinoma; KIRC, kidney renal clear cell carcinoma; UCEC, uterine corpus endometrioid carcinoma; LUSC, lung squamous cell carcinoma; TNBC, triple-negative breast cancer. E, OS durations in patients with uterine cancer with *Notch3* alterations and without *Notch* alterations (amplification and upregulation).

to Spearman correlation analysis. Notch3 overexpression was also significantly correlated with the GATA2 and C/EBP transcription factors based on Spearman correlation analysis (Supplementary Table S3). Importantly, we identified a significant correlation between Jagged-1 and Notch3 expression in HGS-OvCa samples as well as in breast, uterine, and kidney cancers (Fig. 2D; Supplementary Fig. S1B; Table 1). *Notch3* amplification and upregulation were also significantly correlated with shorter survival in patients with uterine cancer (median OS duration, 56 months); patients without these alterations were still alive at the end of this study (P = 0.0008; Fig. 2E).

Biologic effects of Notch3 and cleaved Notch3 in cancer cells

We first used Western blot analysis to screen a panel of OvCa cell lines for expression of Notch family members (Fig. 3A and B). We selected both cleaved Notch3 (NICD3)-positive (OVCAR3, OVCAR5, and A2780) and NICD3-negative (SKOV3, SKOV3 TR, and IGROV1) OvCa cells for additional *in vitro* and *in vivo* studies. After transfecting cancer cells with *Notch3* siRNA (Supplementary Fig. S2A), we noticed high levels of apoptosis in the NICD3-positive cells (Fig. 3C–E), but not in the NICD3-negative cells (Fig. 3F–H); these results suggest that NICD3 expression is an important determinant of the biologic functions of *Notch3* in cancer cells. Furthermore, compared with control cells, anoikis increased greatly in NICD3-positive cells transfected with *Notch3* siRNA (Supplementary Fig. S2B). *Notch3* siRNA also induced cell-cycle arrest in the G_2–M phase in NICD3-positive cells, but not in NICD3-negative cells (Supplementary Fig. S2C).

To determine whether the cleaved Notch3 is a determinant of sensitivity to Notch-targeted therapy, we treated human epithelial OvCa cells (OVCAR5, OVCAR3, SKOV3, HeyA8, and A2780) with a GSI at various concentrations for 72 hours and assessed cell viability. The IC_{50}s of GSI ranged from 3.06 to 7.73 μmol/L. The NICD3-positive cells (A2780, OVCAR3, and OVCAR5) were more sensitive to treatment with GSI than

Table 1. Correlation between Notch3 and Jagged-1 expression in human cancers

Cancer type	Coefficient	*P*	Sample size
HGS-OvCa (Affymetrix microarray)	0.33	3.28E−16	569
HGS-OvCa (Agilent microarray)	0.29	3.48E−12	571
HGS-OvCa (IlluminaRNASeq)	0.46	2.09E−22	411
HNSC	0.08	0.16677	303
LGG	0.50	<0.0000001	174
BRCA-TNBC	0.28	0.002831	112
BRCA-ER$^-$	0.33	4.8E−05	149
BRCA-ER$^+$	0.46	<0.000001	511
BRCA-PR$^-$	0.31	4.65E−06	215
BRCA-PR$^+$	0.51	<0.0000001	443
BRCA-HER2$^-$	0.41	<0.0000001	582
BRCA-HER2$^+$	0.5	4.54E−07	95
CRC	0.13	0.035451	264
KIRC	0.73	3.17E−78	470
UCEC	0.42	0.000001	333
LUSC	0.37	2.27–08	223

Abbreviations: BRCA, breast invasive carcinoma; CRC, colon and rectum adenocarcinoma; HNCS, head and neck squamous cell carcinoma; LGG, brain low-grade glioma; LUSC, lung squamous cell carcinoma; KIRC, kidney renal clear cell carcinoma; TNBC, triple-negative breast cancer; UCEC, uterine corpus endometrioid carcinoma.

were the NICD3-negative cells (SKOV3 and HeyA8; Fig. S2D). GSI-based treatment induced substantially more apoptosis in the NICD3-positive cells than in the NICD3-negative cells (Supplementary Fig. S2E).

Because *Notch3* siRNA arrested cells in the G_2–M phase, we examined whether *Notch3* siRNA could enhance sensitivity to paclitaxel. We found that silencing *Notch3* significantly enhanced the sensitivity of OVCAR3 cells to treatment with paclitaxel ($P < 0.01$; Supplementary Fig. S2F–S2G)

Dynamin-dependent endocytosis is required for Jag1-mediated Notch3 activation

Next, we considered potential explanations for selective cleaved Notch3 expression in cancer cell lines. Given the role of the gamma-secretase complex (*PSEN1*, *APH1A*, *NCSTN*, *APH1B*, and *PSENEN*) in Notch proteolysis, we first used qRT-PCR to examine the expression of the gamma-secretase complex in the panel of OvCa cells. These five genes were not differentially expressed between the NICD3-positive or -negative cells (Supplementary Fig. S3). Because there was no association between the gamma-secretase complex and cleaved Notch3 expression, we next used TCGA data and the Spearman rank correlation coefficient to analyze the relationship between *Notch3* and its potential ligands in patients with HGS-OvCa. There was a significant correlation between Notch3 and Jagged-1 expression in HGS-OvCa as well as other cancers, including cancers of the uterus, breast, and kidney ($P < 0.0001$; Table 1). Therefore, we next evaluated whether Jagged-1 stimulation could induce Notch3 proteolysis in NICD3-negative SKOV3 cells. Whereas treatment with recombinant human Jagged-1 (rhJagged-1; 10 μg/mL) at 48 hours increased cleaved Notch3 expression in these cells compared with controls (Fig. 4A), *Jagged-1* silencing did not decrease cleaved Notch3 levels in NICD3-positive cells (Fig. 4B).These findings prompted us to consider whether endocytosis may be involved in Notch3 activation.

To determine whether endocytosis is involved in Notch3 proteolysis, OVCAR3 cells were treated with dynasore, a cell-permeable inhibitor of dynamin. Cleaved Notch3 expression was decreased in a time- and dose-dependent manner (Fig. 4C and D). Dynasore treatment indeed increased the expression of full Notch3 expression at lower doses and at 1 to 24 hours, likely due to its rapid effect on inhibiting Notch3 receptor degradation, but this treatment decreased full Notch3 and Jagged-1 at higher doses and 48 hours (Fig. 4C and D and Supplementary Fig. S4A). Importantly, dynasore prevented Jagged-1–stimulated cleaved Notch3 expression in the NICD3-negative cells (SKOV3 cells, HeyA8, and 2774), suggesting that endocytosis was required for Jagged-1–mediated Notch3 activation (Fig. 4E; Supplementary Fig. S4B). Next, to identify which dynamins are involved in this endocytotic process to activate Notch3, we screened a panel of OvCa cells for expression of DNM1, DNM2, and DNM3. Among these, DNM1 and DNM2 were expressed in all the cells tested, but DNM3 was present only in some cells (Supplementary Fig. S4C). We then treated the OVCAR3 cells with *DNM1*, *DNM2*, or *DNM3* siRNA or pools of two or three of these dynamin siRNAs (Supplementary Table S4 and Supplementary Fig. S4D). Treatment with the pools of three dynamin siRNAs resulted in much lower cleaved expression in the OVCAR3 cells than did treatment with the individual siRNA duplexes (Fig. 4F), demonstrating that dynamin-dependent endocytosis was a critical determinant of Notch3 activation.

To determine whether inhibiting dynamin-mediated endocytosis *via* dynasore could affect apoptosis, NICD3-positive

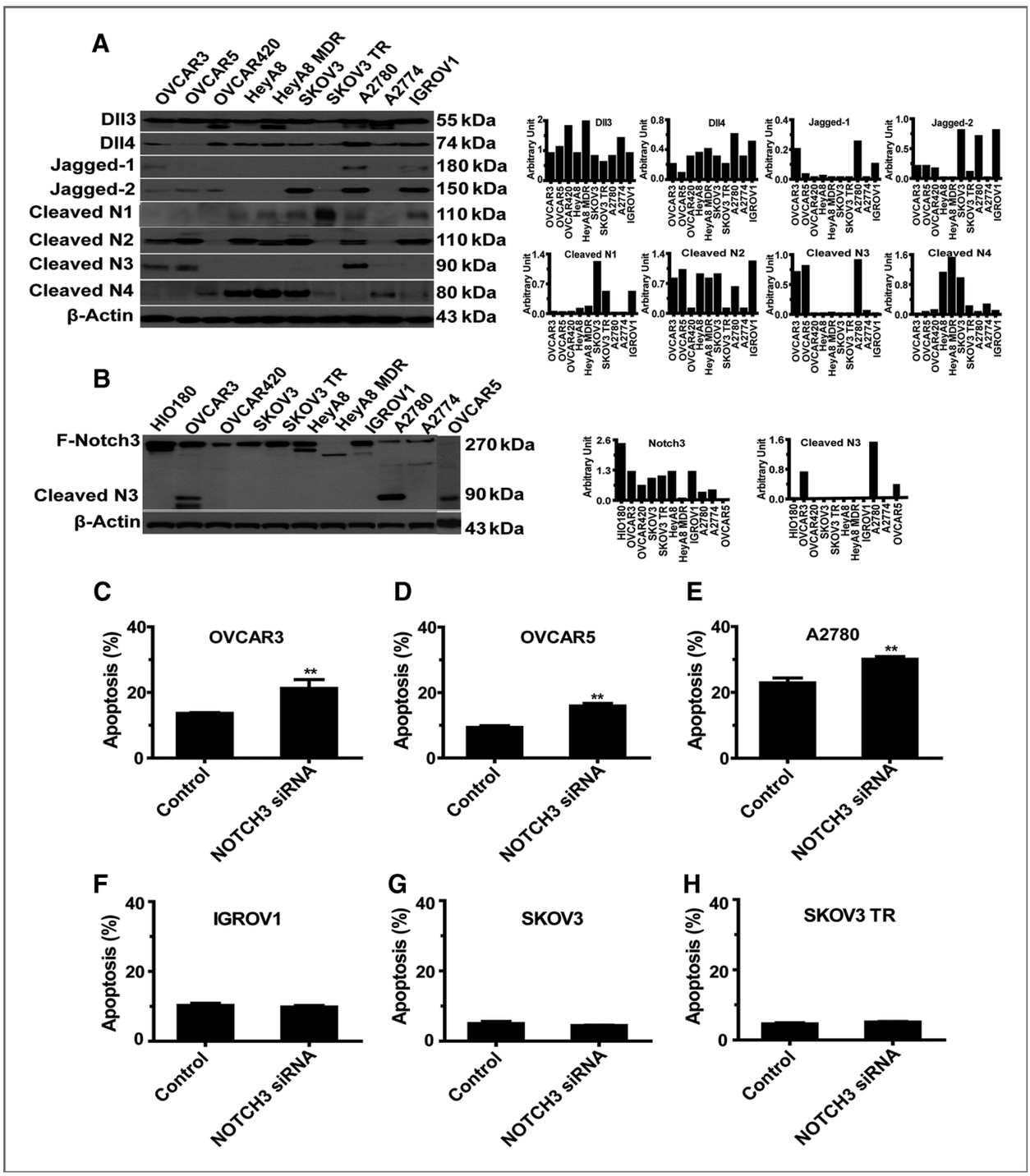

Figure 3. *In vitro* functional studies of *Notch3* silencing. A, Western blot analysis of expression of 8 Notch family proteins in a panel of 10 ovarian cancer (OvCa) cell lines. B, Western blot analysis of expression of full-length Notch3 and cleaved Notch3 (NICD) in a panel of 10 ovarian cancer cell lines. C–H, apoptosis in ovarian cancer cells (NICD3-positive: OVCAR5, OVCAR3, and A2780; NICD3-negative: IGROV1, SKOV3, and SKOV3 TR) after exposure to control siRNA or *Notch3* siRNA for 72 hours; **, $P < 0.01$.

cells (OVCAR5, OVCAR3, and A2780) and NICD3-negative cells (SKOV3) were treated with dynasore (60 μmol/L) for 72 hours. Induction of apoptosis was significantly higher in the Jag1/NICD3-positive cells (A2780 and OVCAR3) than in the Jagged-1/NICD3-negative cells (SKOV3; Fig. 5A; $P < 0.001$). Apoptosis was only slightly increased in the NICD3-positive OVCAR5 cells

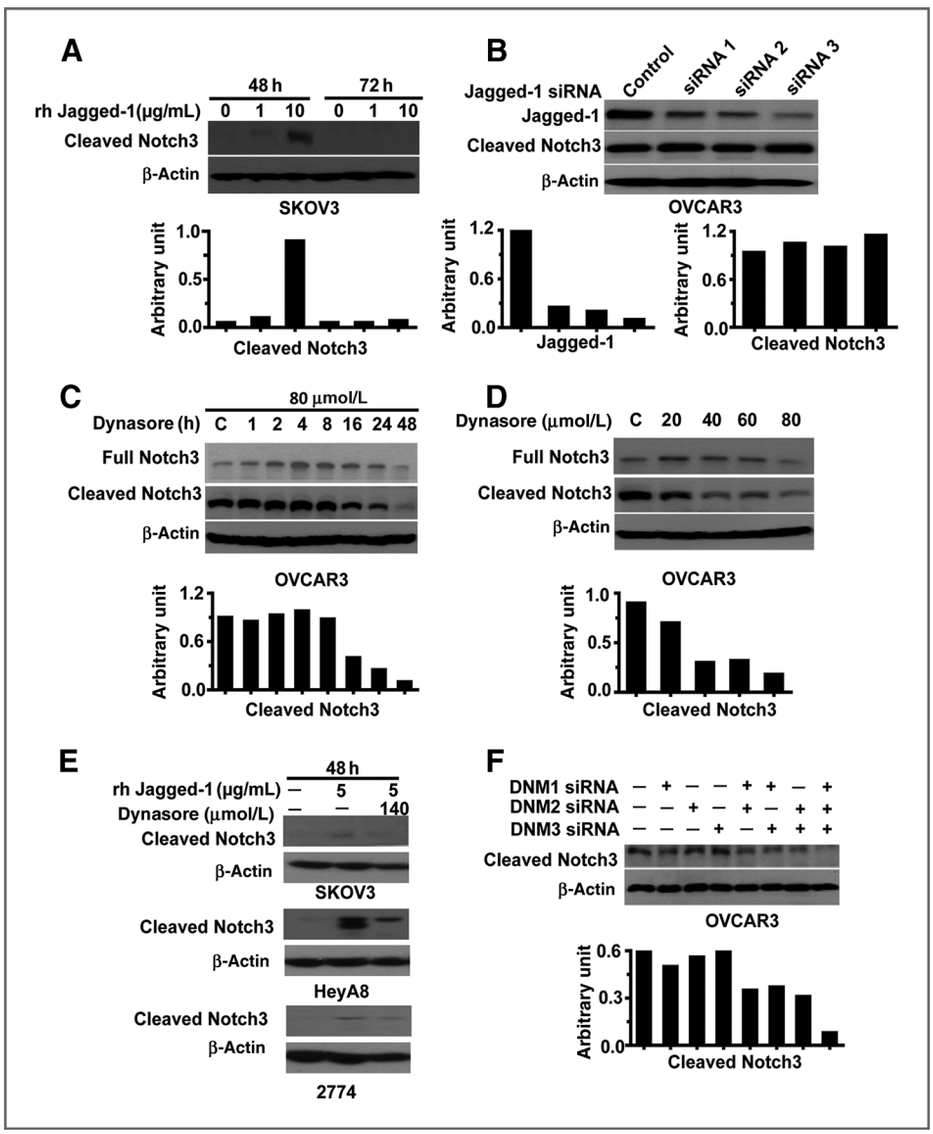

Figure 4. Notch3 activation by dynamin (DNM)-dependent endocytosis. A, effect of Jagged-1 stimulation on Notch3 activation in SKOV3 cells. B, effect of *Jagged-1* silencing on Notch3 activation in OVCAR3 cells. C and D, effect of treatment with dynasore on Notch3 activation in OVCAR3 cells at different time points and doses. E, effect of treatment with dynasore on Jagged-1–mediated Notch3 activation in NICD3-negative ovarian cancer cells (SKOV3, 2774, and HeyA8). F, effect of dynamin silencing on Notch3 activation in OVCAR3 cells.

treated with dynasore, likely because of the weak expression of Jagged-1 in these cells (Fig. 5A). Induction of apoptosis by Dynasore treatment was also noted in uterine cancer cells (Ishikawa), which express Notch3 and Jagged-1 (Supplementary Fig. S4E and S4F). Dynasore treatment increased Jagged-1 expression in uterine cancer cells (Supplementary Fig. S4E), which may occur due to a possible feedback loop of Notch inhibition or cross-talk with other pathways such as Wnt/β-catenin.

Next, we searched for potential Notch3-targeted genes that could be involved in apoptosis in OvCa cells by hierarchical clustering analysis following *Notch3* silencing. There were 461 genes differentially expressed in the OVCAR3 cells following *Notch3* silencing, when defined as a fold change > 0.7 (Supplementary Table S4). Given the robust induction of apoptosis in NICD3-positive cells, a pathway analysis focusing on apoptosis was performed. Among the 56 genes in this pathway, *RPS6KB1* expression was particularly downregulated in response to *Notch3* silencing (Fig. 5B). Moreover, dynasore treatment decreased RPS6KB1 expression by 3.0- and 1.3-fold in OVCAR3 and A2780 cells, respectively (Fig. 5C); we found that cleaved poly ADP ribose polymerase dramatically increased in OVCAR3 and A2780 cells, but not in SKOV3 cells, suggesting that RPS6KB1 was a dominant downstream target of the Notch3 pathway involved in apoptosis. Because it has been reported that PI3K/AKT/mTOR signaling could be modulated by direct repression of PTEN *via* the Notch target gene *Hes1* or *cMyc* (12), we tested *cMyc* and *HES1* in these cells following dynasore treatment. Dynasore treatment decreased cMyc and HES1 levels by 2-fold in the OVCAR3 and A2780 cells, but not in the NICD3-negative cells (Fig. 5C and D).

We also validated the target modulation *in vivo* by examining the effects of Dynasore on expression of Jagged-1, cleaved Notch3, HES1, and RP6SKB1 in the A2780 model. After two i.p.

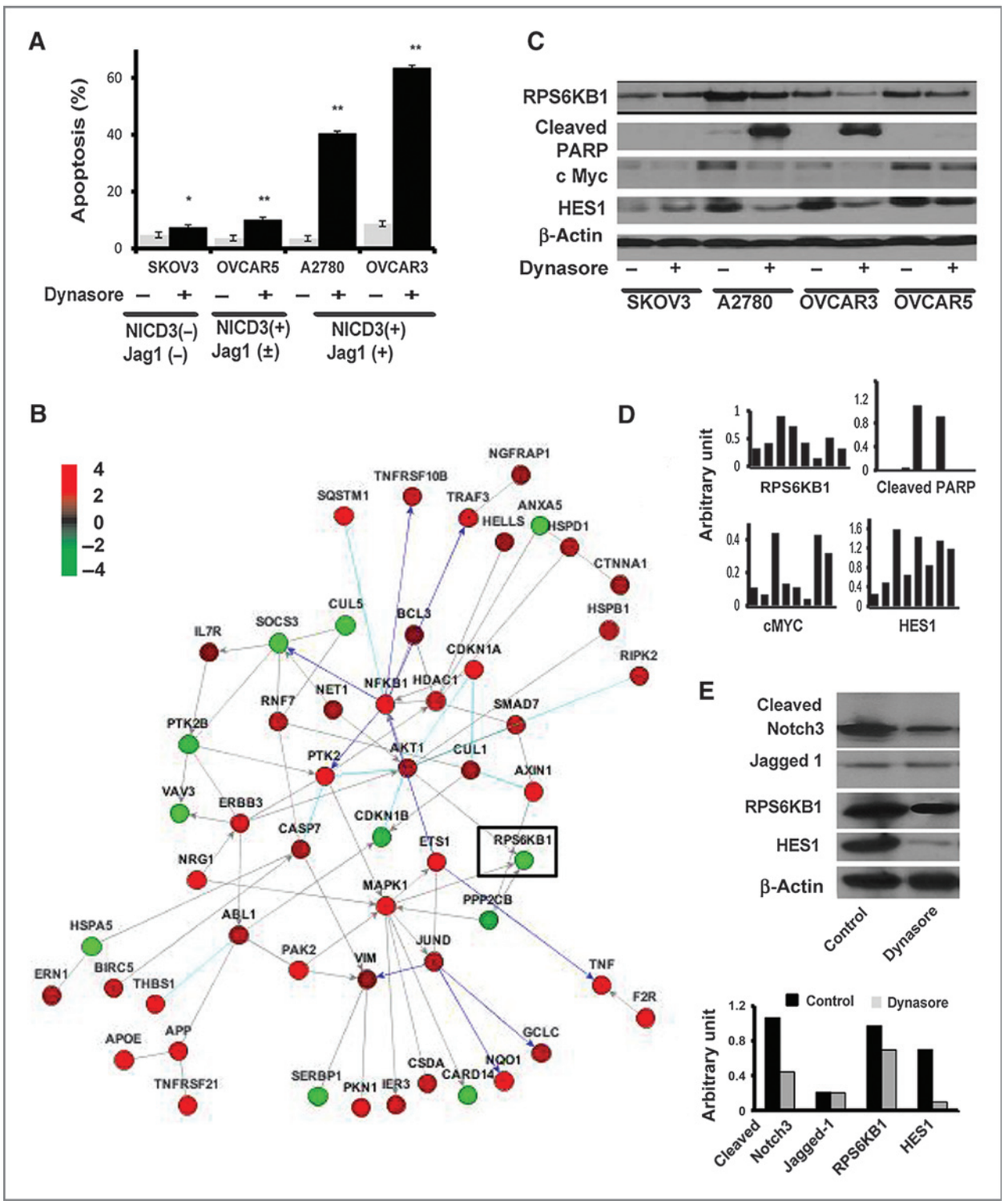

Figure 5. Microarray analysis of Notch3-targeted genes in ovarian cancer cells. A, analysis of apoptosis in NICD3-positive and NICD3-negative cells after exposure to dynasore for 72 hours. *, $P < 0.05$; **, $P < 0.01$. B, pathway analysis of apoptosis-related genes in OVCAR3 cells treated with *Notch3* siRNA or control siRNA. C and D, Western blot and image analysis of *RPS6KB1*, cleaved *PARP*, *cMyc*, and *Hes-1* in ovarian cancer cells treated with dynasore. E, Western blot analysis of target modulation (cleaved Notch 3, HES1, Jagged-1, and RPS6KB1) in tumor tissues obtained from the *in vivo A2780* model. Ovarian cancer cells were injected intraperitoneally into the mice. Three weeks later, the mice were randomly allocated to two treatment groups ($n = 5$/group): (i) control, (ii) dynasore.

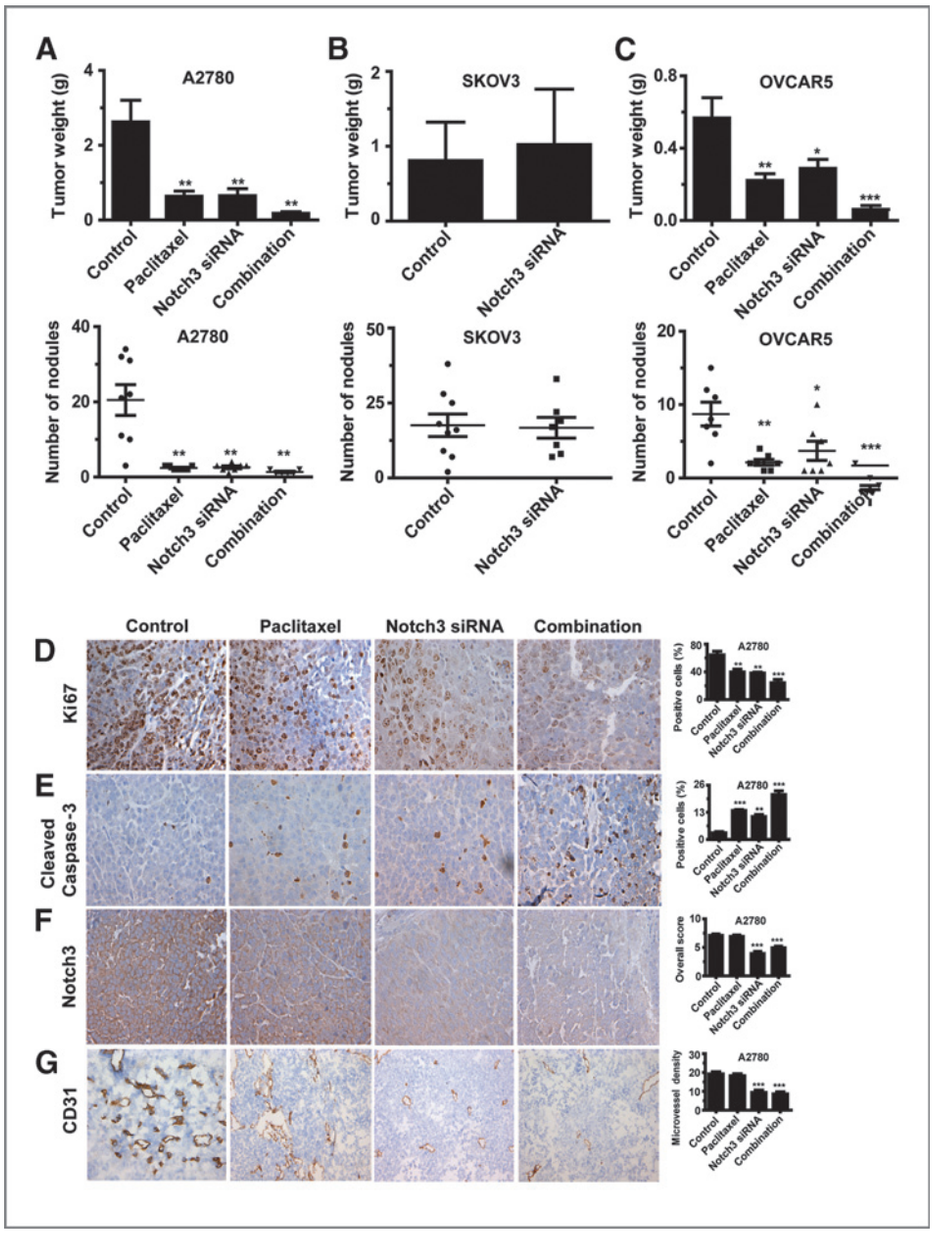

Figure 6. *In vivo* study of *Notch3* siRNA in mouse models of ovarian cancer (OvCa). A–C, effect of treatment with *Notch3* siRNA and/or paclitaxel on tumor weight in NICD3-positive models (OVCAR5 and A2780) and the NICD3-negative model (SKOV3). Error bars, SEM. *, $P < 0.05$; **, $P < 0.01$; ***, $P < 0.001$. D–G, effect of *Notch3* siRNA and/or paclitaxel on biologic endpoints: cell proliferation (Ki67 expression), apoptosis (cleaved caspase-3 expression), Notch3 expression and microvessel density (CD31). Original magnification, ×200. Error bars, SEM; *, $P < 0.05$; **, $P < 0.01$; ***, $P < 0.001$.

injections of dynasore (60 mg/kg), cleaved Notch3, HES1, and RP6SKB1 levels, but not Jagged-1, were decreased in tumors treated with Dynasore (Fig. 5E).

In vivo targeting of Notch3 with siRNAs

On the basis of our *in vitro* findings, we next tested whether silencing *Notch3* could induce apoptosis *in vivo* and enhance sensitivity of cancer cells to chemotherapy. For *in vivo* testing, the A2780 (NICD3/Jagged-1–positive) and SKOV3 (NICD3/Jagged-1–negative) models were used. For systemic delivery of siRNA, the well-characterized CH delivery system (8) was used. In the A2780 model, tumors treated with *Notch3* siRNA-CH or paclitaxel alone weighed 74.1% ($P = 0.0093$) and 75.7% ($P = 0.0081$) less, respectively, than control siRNA-CH–treated tumors (Fig. 6A). Combining *Notch3* siRNA-CH and paclitaxel reduced tumor weight by 99.3% ($P = 0.003$, compared with tumor weight in control mice). Mice receiving this combination treatment also had significantly fewer tumor nodules on average than did control siRNA-CH–treated mice ($P = 0.001$). In the SKOV3 model, *Notch3* silencing did not affect tumor weight or the number of tumor nodules (Fig. 6B). Treatment with *Notch3* siRNA-CH did not significantly affect body weight (Supplementary Fig. S5A). In the OVCAR5 (NICD3-positive) model, tumors treated with *Notch3* siRNA-CH or paclitaxel alone weighed 49.1% ($P = 0.0432$) and 60.7% ($P = 0.013$) less, respectively, than did the control siRNA-CH tumors (Fig. 6C). Also, combining *Notch3* siRNA-CH and paclitaxel decreased tumor weights by 78.7% and 72.3%, respectively, from weights

with either treatment alone ($P = 0.001$ and 0.003, respectively). Body weight was not significantly affected by treatment (Supplementary Fig. S5A).

Notch3 levels were significantly decreased in the *Notch3* siRNA-CH-treated groups compared with the levels in the untreated mice ($P < 0.01$). In the A2780 model, apoptosis was significantly higher in the tumors treated with *Notch3* silencing than in untreated cells (Fig. 6D–G, $P < 0.01$). Compared with the controls, proliferation and angiogenesis were significantly decreased in the tumors treated with the combination therapy. Similar effects were noted in the OVCAR5 model ($P < 0.01$; Supplementary Fig. S5B–S5E).

Discussion

The key findings from our work are that Notch pathway alterations are prevalent and significantly related to poor clinical outcome in patients with ovarian cancer. Particularly, *Notch3* alterations, including amplification and upregulation, were highly associated with poor survival. Targeting *Notch3* inhibited the growth of ovarian cancer and induced apoptosis. Importantly, we found that dynamin-mediated endocytosis was required for selectively activating Jag1-mediated Notch3 signaling. Cleaved Notch3 expression was the critical determinant of response to Notch-targeted therapy. Collectively, these data identify previously unknown mechanisms underlying Notch3 signaling and identify new, biomarker-driven approaches for therapy.

Why Notch3 expression is preferentially upregulated in patients with ovarian cancer is not clear. Several mechanisms may contribute to its upregulation. *Notch3* upregulation was partially correlated with its amplification; Notch3 expression may be caused by transcriptional activation or loss of negative regulators such as *SNW1*, because the ability of NICD3 to recruit coactivators and corepressors and undergo conformational changes is different from that of *Notch1* and *Notch2* (13). However, we cannot rule out a role for *SNW1* in the negative regulation of Notch3 pathway activation in such cases (14). Unlike the proteolysis findings with Notch1, Notch2, and Notch4, we found that Notch3 proteolysis was selectively activated in ovarian cancer cells. We considered potential explanations for selective cleaved Notch3 expression in ovarian cancer cells, such as differential expression of the gamma-secretase complex in NICD3-positive and NICD3-negative ovarian cancer cells, preferential pairing of ligands and Notch3, and ligand endocytosis for signaling activation and receptor degradation. Our data did not support an association between the gamma-secretase complex and cleaved Notch3 expression in NICD3-positive versus -negative ovarian cancer cells. It has been suggested that preferential pairing of Notch3 and Jagged-1 or DLL4 can occur in colon cancer cells (13). We found that Notch3 proteolysis was selectively activated in ovarian cancer cells in a Jagged-1–dependent manner, which highlights a critical role for Jagged-1 in activating Notch3 signaling. Jagged-1 expression has also been reported to be regulated directly by Notch 3 and Wnt/β-catenin in ovarian cancer, which might contribute to maintaining long-term Notch3 signaling activation in cancer cells (15).

The exact function of ligand endocytosis in intracellular signaling is unknown. Two possible models have been reported: one that involves ligand-induced Notch signaling (16–18) and another that involves alternative endocytotic adaptors such as dynamin, epsins, and actin (17). Before our work, role of endocytotic adaptors in Jagged-1–mediated endocytosis in activating Notch3 in ovarian cancer was unknown. Three different dynamin genes have been identified in mammals, including DNM1, DNM2, and DNM3. Dynamin has been reported as an endocytotic adaptor that functions in membrane tabulation and fission of budding vesiculo–tubular structures and regulates ligand internalization (19). We demonstrated that selective Notch3 activation is dependent on dynamin-mediated endocytosis and blocking dynamins with dynamin inhibitor significantly increased apoptosis in ovarian cancer, which represents an innovative strategy for inhibiting Notch3 activation.

Taken together, our findings demonstrate that Notch pathway alterations, especially in *Notch3* (amplification or upregulation of expression), are prevalent in HGS-OvCa cases and shorten OS durations. Cleaved Notch3 is a key determinant of *Notch3* biology, and dynamin-mediated endocytosis is required for Jagged-1–mediated Notch3 activation. Targeting Notch3 pathway activation with dynamin inhibitors (20) combined with paclitaxel could be considered for future clinical investigation.

Disclosure of Potential Conflicts of Interest

No potential conflicts of interest were disclosed.

Authors' Contributions

Conception and design: W. Hu, T. Liu, J. Bottsford-Miller, S.Y. Wu, S.L. Tucker, G. Lopez-Berestein, A.K. Sood

Development of methodology: W. Hu, H.J. Dalton, J. Bottsford-Miller, A.K. Sood

Acquisition of data (provided animals, acquired and managed patients, provided facilities, etc.): J. Huang, T. Miyake, H.J. Dalton, R. Rupaimoole, H.D. Han, J. Bottsford-Miller, Y. Kang, A.K. Sood

Analysis and interpretation of data (e.g., statistical analysis, biostatistics, computational analysis): W. Hu, C. Ivan, Y. Sun, T. Miyake, R. Rupaimoole, J. Bottsford-Miller, C.V. Pecot, J.-S. Lee, P. Ram, K.A. Baggerly, R.L. Coleman, A.K. Sood

Writing, review, and/or revision of the manuscript: W. Hu, T. Liu, L.S. Mangala, T. Miyake, H.J. Dalton, B. Zand, A.M. Nick, S.L. Tucker, S.L. Tucker, G. Lopez-Berestein, R.L. Coleman, A.K. Sood

Administrative, technical, or material support (i.e., reporting or organizing data, constructing databases): W. Hu, J. Huang, J. Liu, S.L. Tucker, G. Lopez-Berestein, A.K. Sood

Study supervision: W. Hu, A.K. Sood

Network Analyses: V. Sehgal

Acknowledgments

The authors thank Nicholas B. Jennings for technical support and Diane Hackett and Jill Delsigne, Department of Scientific Publications, for editing the article.

Grant Support

This work were was supported in part by the NIH (grants P50 CA083639, CA109298, P50 CA098258, UH2 TR000943, CA128797, RO1 CA177909, and U54 CA151668), the Ovarian Cancer Research Fund (a Program Project Development Grant), the United States Department of Defense (grants OC120547 and OC093146), the Zarrow Foundation, the Marcus Foundation, the Chapman Foundation, the Meyer and Ida Gordon Foundation #2, the Betty Anne Asche Murray Distinguished Professorship, MD Anderson Cancer Center Support

Grant CA016672, the Gilder Foundation, and the RGK Foundation. J. Bottsford-Miller, B. Zand, R.A. Previs, and H.J. Dalton were supported by a National Cancer Institute/United States Department of Health and Human Services/NIH Training grant (T32 CA101642). W. Hu was partially supported by the Gynecologic Cancer Foundation/Florence and Marshall Schwid Ovarian Cancer Award.

The costs of publication of this article were defrayed in part by the payment of page charges. This article must therefore be hereby marked *advertisement* in accordance with 18 U.S.C. Section 1734 solely to indicate this fact.

Received July 19, 2013; revised February 11, 2014; accepted March 18, 2014; published OnlineFirst April 17, 2014.

References

1. Chan YM, Jan YN. Roles for proteolysis and trafficking in notch maturation and signal transduction. Cell 1998;94:423–6.
2. Artavanis-Tsakonas S, Muskavitch MA. Notch: the past, the present, and the future. Curr Top Dev Biol 2010;92:1–29.
3. Wang Z, Li Y, Ahmad A, Azmi AS, Banerjee S, Kong D, et al. Targeting Notch signaling pathway to overcome drug resistance for cancer therapy. Biochim Biophys Acta 2010;1806:258–67.
4. TCGA Research Group. Integrated genomic analyses of ovarian carcinoma. Nature 2011;474:609–15.
5. Cooke SL, Brenton JD. Evolution of platinum resistance in high-grade serous ovarian cancer. Lancet Oncol 2011;12:1169–74.
6. Landen CN Jr, Birrer MJ, Sood AK. Early events in the pathogenesis of epithelial ovarian cancer. J Clin Oncol 2008;26:995–1005.
7. Saad AF, Hu W, Sood AK. Microenvironment and pathogenesis of epithelial ovarian cancer. Horm Cancer 2010;1:277–90.
8. Lu C, Han HD, Mangala LS, Ali-Fehmi R, Newton CS, Ozbun L, et al. Regulation of tumor angiogenesis by EZH2. Cancer Cell 2010;18:185–97.
9. Smyth GK. Limma: linear models for microarray data. In Bioinformatics and computational biology: solutions using R and bioconductor. New York, NY:Springer; 2005.
10. Eisen MB, Spellman PT, Brown PO, Botstein D. Cluster analysis and display of genome-wide expression patterns. Proc Natl Acad Sci U S A 1998;95:14863–8.
11. Komurov K, Dursun S, Erdin S, Ram PT. NetWalker: a contextual network analysis tool for functional genomics. BMC Genomics 2012;13:282.
12. Wong GW, Knowles GC, Mak TW, Ferrando AA, Zuniga-Pflucker JC. HES1 opposes a PTEN-dependent check on survival, differentiation, and proliferation of TCRbeta-selected mouse thymocytes. Blood 2012;120:1439–48.
13. Serafin V, Persano L, Moserle L, Esposito G, Ghisi M, Curtarello M, et al. Notch3 signalling promotes tumour growth in colorectal cancer. J Pathol 2011;224:448–60.
14. Bellavia D, Checquolo S, Campese AF, Felli MP, Gulino A, Screpanti I. Notch3: from subtle structural differences to functional diversity. Oncogene 2008;27:5092–8.
15. Chen X, Stoeck A, Lee SJ, Shih Ie M, Wang MM, Wang TL. Jagged1 expression regulated by Notch3 and Wnt/beta-catenin signaling pathways in ovarian cancer. Oncotarget 2010;1:210–8.
16. Yamamoto S, Charng WL, Bellen HJ. Endocytosis and intracellular trafficking of Notch and its ligands. Curr Top Dev Biol 2010;92:165–200.
17. Meloty-Kapella L, Shergill B, Kuon J, Botvinick E, Weinmaster G. Notch ligand endocytosis generates mechanical pulling force dependent on dynamin, epsins, and actin. Dev Cell 2012;22:1299–312.
18. Le Borgne R, Bardin A, Schweisguth F. The roles of receptor and ligand endocytosis in regulating Notch signaling. Development 2005;132:1751–62.
19. Kirchhausen T, Macia E, Pelish HE. Use of dynasore, the small molecule inhibitor of dynamin, in the regulation of endocytosis. Methods Enzymol 2008;438:77–93.
20. Masaike Y, Takagi T, Hirota M, Yamada J, Ishihara S, Yung TM, et al. Identification of dynamin-2-mediated endocytosis as a new target of osteoporosis drugs, bisphosphonates. Mol Pharmacol 2010;77:262–9.